Am J Transl Res 2016;8(12):5519-5531
www.ajtr.org /ISSN:1943-8141/AJTR0040070

Original Article

Picroside II protects against sepsis via suppressing inflammation in mice

Ying Huang[1,2*], Miao Zhou[2*], Chengbao Li[4*], Yuanli Chen[1], Wei Fang[4], Guo Xu[5], Xueyin Shi[1,2,3]

[1]Jiangsu Province Key Laboratory of Anesthesiology and Jiangsu Province Key Laboratory of Anesthesia and Analgesia Application Technology, Xuzhou Medical University, Xuzhou, China; [2]Department of Anesthesiology and SICU, Xinhua Hospital, School of Medicine, Shanghai Jiaotong University, Shanghai, China; [3]Department of Anesthesiology, Changzheng Hospital, Second Military Medical University, Shanghai, China; [4]Department of Medicine, Hebei North University, Zhangjiakou, Hebei, China; [5]Department of General Surgery, Huai'an First People's Hospital, Nanjing Medical University, Huai'an, China. [*]Equal contributors.

Received August 31, 2016; Accepted November 5, 2016; Epub December 15, 2016; Published December 30, 2016

Abstract: Picroside II, an iridoid compound extracted from Picrorhiza, exhibits anti-inflammatory and anti-apoptotic activities. We explored the protective effects and mechanisms of picroside II in a mouse model of sepsis induced by cecal ligation and puncture (CLP), using three groups of mice: Group A (sham), Group B (CLP+NS) and Group C (CLP+20 mg/kg picroside II). The mortality in mice with sepsis was decreased by the administration of picroside II, and lung injury was alleviated simultaneously. Picroside II treatment enhanced bacterial clearance in septic mice. Further, picroside II treatment alleviated the inflammatory response in sepsis and enhanced immune function by inhibiting the activation of NLRP3 inflammasome and NF-κB pathways. Picroside II may represent an anti-inflammatory drug candidate, providing novel insight into the treatment of sepsis.

Keywords: Picroside II, sepsis, inflammation, NF-κB pathways, NLRP3, apoptosis

Introduction

Sepsis is a complex inflammatory syndrome induced by pathogens and their toxic products. Absence of prompt medical treatment results in severe sepsis, septic shock and multiple organ dysfunction syndrome (MODS) [1, 2]. Currently, approximately 800,000 cases of sepsis are estimated to occur annually in the USA with a mortality rate of about 27% [3]. Despite advances in medical treatment worldwide, humans are increasingly susceptible to microbial diseases. Moreover, the pathophysiology of sepsis is complex and difficult to treat. Consequently, it is a great clinical challenge. The pathophysiology of sepsis is characterized by excessive inflammatory reaction (namely "the storm of inflammation") and secondary immune disorder or immune function inhibition (namely "immunosuppressive phase") [4, 5]. The pattern recognition receptors (PRRs), as well as their downstream signaling pathways, mediate strong inflammatory response, activate various inflammatory cells and release a number of proinflammatory factors with excessive catabolism and energy consumption to eliminate pathogens during the storm of inflammation [6]. During the elimination of pathogens, excessive production of inflammatory mediators contributes to overwhelming inflammatory response, which triggers systemic inflammatory response syndrome (SIRS), and tissue and cell damage [7]. Thus, it is crucial to control the damage associated with excessive inflammation to effectively ameliorate sepsis.

Studies suggest that specific herbal ingredients in traditiional Chinese medicine (TMC) play an effective role in treating sepsis. Studies have shown that iridoids such as geniposide, artemisinin and paeoniflorin present in medicinal herbs improve the systemic inflammatory status of mice with sepsis by compromising the bacterial endotoxin (LPS), inhibiting the excessive release of inflammatory mediators, and improving microcirculation and immune regulation [8-10]. Picroside II is an iridoid compound utilized in TMC. Currently, three iridoids have

been isolated from *Picrorhiza scrophularii flora pennell* including picroside II, picroside II, and picroside III. Picroside II is the most abundant iridoid, which is the primary effective component [11]. According to Jian-Wen et al., picroside II directly reduced the production of ROS to improve the activities of antioxidant enzymes by inhibiting free radical reactions, and promoting the recovery of injured cells, to protect PC12 cells from glutamate-induced damage [12]. Lei et al. found that injecting picroside II into rat tail vein or intraperitoneal cavity significantly decreased the production of reactive oxygen species and inflammatory factors in renal ischemia reperfusion injury, in addition to inhibiting the expression of TLR, NF-κB and I-κB and reducing cellular apoptosis [13]. Wei et al. showed that picroside II reduced airway inflammation [14]. Therefore, evidence suggests that picroside II is anti-inflammatory, and alleviates oxidative stress and damage. Consequently, our study concluded that picroside II plays a key anti-inflammatory role in sepsis.

NF-κB, known as nuclear factor-κB, is found in almost all the cell types. Exogenous injury or exposure to bacterial toxins activates NF-κB expression [15]. The NF-κB activating pathways are very complex and are mediated via diverse signal transduction pathways in cells. Primarily, various stimulating signals bind to membrane receptors and are translocated into the cytoplasm, to activate the inhibitor of nuclear factor kappa-B kinase (IKK). IKK complex specifically phosphorylates the I-κB. The phosphorylated IκB dissociates from NF-κB, rapidly triggering the degradation of ubiquitin proteasome system. IκB, released from NF-κB, is translocated rapidly into the nucleus, to combine with the κB promoter and enhancer sequences of the target gene, to trigger the expression of cytokines, adhesion molecules, inflammatory reaction enzymes and MHC [16, 17]. The activation of NF-κB pathway is closely related to the systemic inflammatory response syndrome (SIRS) induced by sepsis. Clinical studies showed that NF-κB activity in the peripheral monocytes and neutrophils of patients with SIRS was significantly higher than in the healthy control group, and is a prognostic indicator of sepsis [18]. The NF-κB activity of neutrophils in patients with postoperative complications such as MODS was higher than in patients without any complications. Therefore, NF-κB activation mediates the pathophysiology of organ injury and uncontrolled inflammatory reaction [19].

Inflammasome is an important multiprotein complex required for pathogen elimination, as well as oxidative stress after sepsis in immune cells [20]. Activation of macromolecular protein complex induces self-aggregation of inactive pro-caspase-1 and hydrolysis into caspase-1 [21]. Caspase-1 is the major rate-limiting enzyme in the conversion of the precursors of pro-inflammatory cytokines IL-1β and IL-18 to their active forms [22]. However, caspase-1 induces proinflammatory form of cell death known as pyroptosis after activation [23].

As a member of inflammasome, NLRP3 inflammasome senses the pathogen-associated molecular pattems (PAMPs) of bacteria, viruses, and fungi to trigger inflammatory response [24]. Activated NLRP3 inflammasome induces the maturation and secretion of IL-1β and IL-18, which recruit inflammatory cells to infectious or injuryed sites [25]. Therefore, NLRP3 inflammasome plays an important role in sepsis induced by microorganisms.

Our study investigated the effect of picroside II on the survival rate, organ injury, transcription factors NF-κB and NLRP3 inflammasome in a mouse model of cecal ligation and puncture (CLP). Furthermore, we discussed the potential mechanism of picroside II in the expression of transcription factors NF-κB and NLRP3 inflammasome.

Materials and methods

Experimental animals

Male C57BL/6 (6-8 weeks old, 18-25 g) mice were purchased from the Animal Lab Center of the Second Military University, and caged in a temperature-controlled (22±2°C) environment under a 12-12 h light-dark cycle with free access to food and water. All the experiments were approved by the Animal Care and Use Committee of the Second Military Medical University (SMMU, Shanghai, China).

Experimental design

To observe the 10-day survival as shown in **Figure 1**, 30 C57BL/6 male mice were randomly divided into three groups (n = 10): Group A

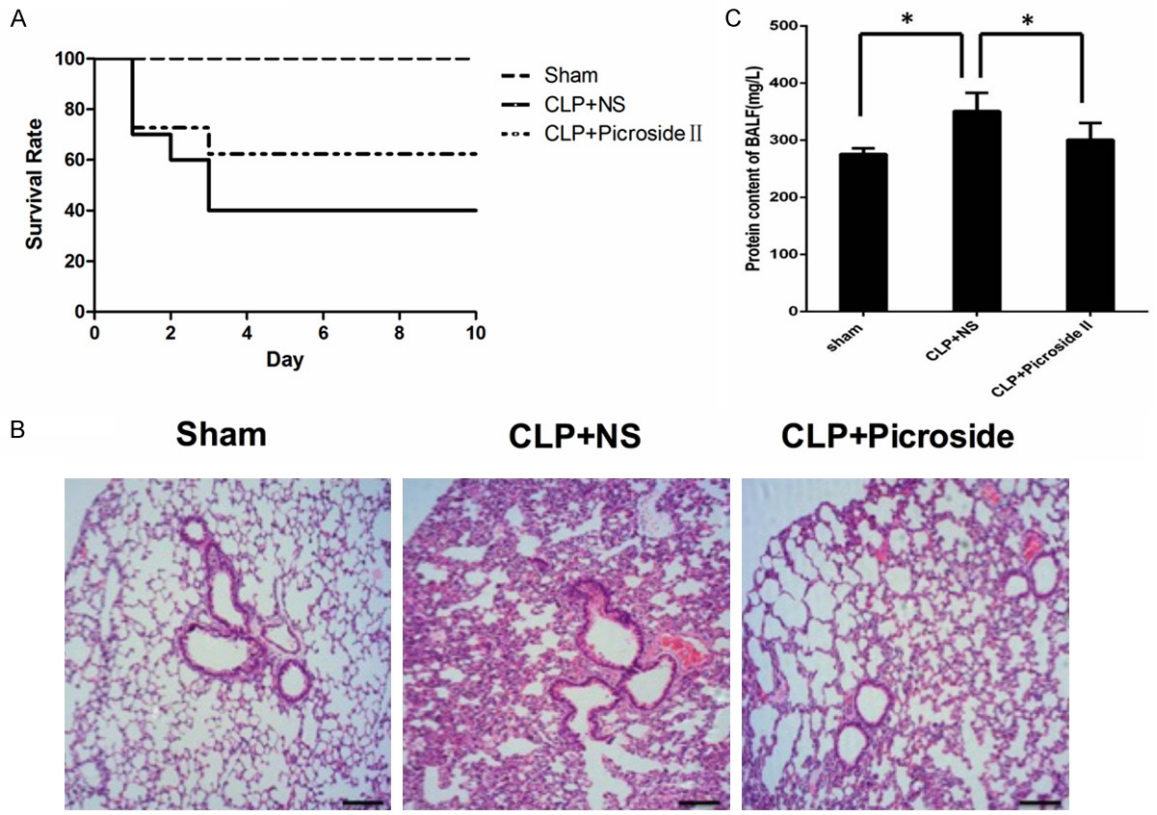

Figure 1. Protective effects of picroside II in mice with sepsis. A: The 10-day survival rate of mice in the three groups. n = 10. B: HE staining revealed pathological changes in lung tissue. Magnification: 100×. C: Protein content in BALF of each group, n = 6. *, P < 0.05. All the bars represent mean ± sd.

(Sham), Group B (CLP+NS), and Group C (CLP+20 mg/kg picroside II). Normal saline (0.9% w/v of NaCl) (NS) and picroside II were injected into mice via tail vein at 2 h, 14 h, 26 h, and 38 h after CLP. Simultaneously, we divided 18 mice into three groups as above, and injected normal saline and picroside II by tail vein at 2 h and 14 h after CLP. We collected bronchoalveolar lavage fluid, lung tissue, peripheral blood and peritoneal lavage fluid at 24 h after CLP.

Sepsis model

The sepsis model was created using the experimental methods of cecal ligation and puncture (CLP) published by Rittirsch D in Nature Protocol [26]. Mice were fasted for 8 h and anesthetized by intraperitoneal injections of 0.75% pentobarbital solution (10 μL/g) before surgery. They were fixed on the operation panel, and after routine disinfection of the abdominal skin, a longitudinal, paramedian incision of 1 cm was created. The subcutaneous tissue layer was separated and the abdominal cavity was opened to locate the cecum. The mesentery at the distal end of cecum and the large intestine was isolated. The cecum was tightly ligated with a No. 3 sterile silk at the 1/2 of distal end. The ligated cecum was penetrated and punctured with sterile needle No. 7 at the center of the distal end, and pushed the cecum back to the abdominal cavity. After closing and suturing the abdominal cavity, mice were injected subcutaneously with 1 mL of NS for fluid resuscitation. The mice were returned to the squirrel-cage after proper labeling. The whole experiment was conducted at room temperature (22--25°C), and the mice were abstained from food and water after surgery. Except for CLP, the remaining steps in the sham-operated mice were similar to the experimental group.

Hematoxylin-eosin staining (HE)

The lungs in the experimental mice were exposed bilaterally and the bilateral rib was extended to cut the thorax after cardiac blood

sampling. Unilateral lung tissue was collected, immersed in 4% paraformaldehyde solution to provide adequate fixation. The tissue was gradually dehydrated by exposure to an ethanol series ranging from low to high concentrations before treatment with xylene. The transparent samples were embedded in molten paraffin, cooled and solidified. The embedded wax blocks were sliced with microtome, affixed to a slide after hot ironing, dried in the oven at 45°C. The slices were deparaffinized using xylene, followed by treatment with ethanol (high to low), and finally distilled water. Slices were stained with hematoxylin solution for 5 min, and separated for 10 s with acidic water and ammonia, washed for 1 h under running water, stained for 3 min using alcohol eosin solution after dehydration for 10 min in an ethanol series (low to high concentration). After treatment with xylene following anhydrous alcohol dehydration, they were covered with glass and sealed with rubber.

Protein concentration in bronchoalveolar lavage fluid (BALF)

The experimental mice were anesthetized with intraperitoneal injection of 0.75% pentobarbital solution (10 μL/g) and fixed on the operation panel after anesthesia. A transverse incision of mouse neck skin was made to expose the trachea. The catheter was inserted into the whole lung and lavaged with 1 mL saline. The lavage fluid was recovered. The procedure was repeated three times to ensure the recovery of more than 80%. Each mouse was exposed to the same volume of fluid. After collection of the BALFs in all the experiments completely, the protein concentration was determined using a protein concentration assay kit according to the instructions.

Detection of bacterial clearance in peripheral blood and peritoneal lavage fluid

Initially, the blood and peritoneal lavage samples were prepared, followed by addition of 100 μL samples to 900 μL saline in a tube. After mixing, 100 μL liquid was drawn from the tube labeled as tube A and transferred to a centrifuge tube containing 900 μL saline, which was labeled as tube B. An aliquot of 100 μL liquid drawn from tube B, was added to a centrifuge tube containing 900 μL saline, which was labeled as tube C. Each sample was diluted into three tubes according to the method described above. The nutrient agar plate containing 4% sterile nutrient agar was used to evenly distribute 100 μL of the pre-diluted sample corresponding to the concentration of the nutrient agar plate with the coater. After incubation for 24 h at 37°C, the colony count was recorded in each agar plate. Bacterial content was estimated in the peripheral blood and peritoneal lavage fluid of the experimental mice according to the number of bacterial colony forming units.

Enzyme-linked immunosorbent assay (ELISA)

The samples (mouse serum or cell supernatant) were reasonably diluted, and the standard solution was diluted from a high to a low concentration gradient. The kit was transferred from 4°C, and equilibrated to room temperature (20-25°C). First, the excess microplate strips were removed from the plate frame, followed by addition of 100 μL of diluted standard or sample to the center of the reaction wells before incubation for 40 min at 37°C. The plate was washed four to six times and the washing buffer was removed. Second, 50 μL of the first antibody solution was added and mixed with distilled water, and incubated for 20 min at 37°C. After repeatedly washing as above, 100 μL of enzyme-labeled antibody working fluid (HRP) was added, and incubated for 10 min at 37°C. Third, the samples were washed again four to six times, followed by addition of 100 μL of substrate working solution, and incubated for 15 min at 37°C in the dark. Finally, a 100 μL of stop buffer was added and mixed well. OD values were read at 450 nm within 30 min. Using the OD value as the ordinate and the standard concentration as the abscissa, the standard curve was drawn. The sample concentration was determined based on the OD value in the standard curve.

Real-time quantitative polymerase chain reaction (qRT-PCR)

After the mice were sacrificed, unilateral lung tissue was obtained immediately and treated with 1 mL TRIzol after trituration, followed by transfer to room temperature for 5 min. The supernatant was obtained after centrifugation at 12000 rpm for 5 min at 4°C, and transferred to the new non-ribozyme EP tubes. Next, 0.2 mL of chloroform was added and oscillated for

15 s. The upper aqueous phase was transferred into a new tube after centrifugation at 12000 rpm for 10 min at 4°C, followed by addition of 1 volume of 70% alcohol and centrifugation at 8000 rpm for 5 min at 4°C, and dried at room temperature or vacuum for 5-10 min. Finally, 50 μL of RNA samples without ribozyme were dissolved in water to measure RNA concentration and reverse transcription by adding a total RNA of 500 ng, 5× PrimeScript RT Master Mix 2 μL and complemented with 10 μL of water lacking ribozyme. Reaction conditions included reverse transcription (3°C, 15 min), inactivation of the reverse transcriptase (85°C, 5 s) and preservation (4°C). Finally, 10 μL of SYBR Premix Ex Taq II was added, followed by 0.8 μL of upstream primer and downstream primers, respectively, 0.4 μL of ROX Reference Dye II, 2 μL of DNA template and 6 μL of sterile distilled water, and mixed uniformly in 96-well PCR plates. A PCR plate was inserted into the automated PCR instrument (7500 system) using the following cycle parameters: initial denaturation (Reps: 1; 95°C 30 s), PCR reaction (Reps: 40; 95°C 5 s; 60°C 34 s) and dissolved phase.

The PCR primer sequences were:

① β-actin forward primer: AGTGTGACGTTGACATCCGT, β-actin reverse primer: GCAGCTCAGTAACAGTCCGC; ② IL-6 forward primer: TAGTCCTTCCTACCCCAATTTCC, IL-6 reverse primer: TTGGTCCTTAGCCACTCCTTC; ③ IL-1β forward primer: GCAACTGTTCCTGAACTCAACT, IL-1β reverse primer: ATCTTTTGGGGTCCGTCAACT; ④ TNF-α forward primer: AAGCCTGTAGCCCACGTCGTA, TNF-α reverse primer: GGCACCACTAGTTGGTTGTCTTTG.

Flow cytometry

Detection of the neutrophil number: Peripheral blood and peritoneal lavage fluid of mice were transferred into the inflow pipes, respectively, in aliquots of 100 μL, followed by the addition of 2 mL of red blood cell lysis buffer (BD555899), vortexed gently and incubated at room temperature for 15 min. The supernatant was discarded after centrifugation at 2000 rpm for 5 min. The cells were resuspended in cold PBS buffer at a concentration of 1×10^7/ml. The horizontal and vertical axes were set, and each parameter was adjusted based on a physical map. Neutrophil population data were analyzed by Flow Jo VX.

Detection of cellular apoptosis: Spleens in each group were extracted and grounded in 200 mesh, into a single cell suspension. The remaining leukocytes were almost lymphocytes after red blood cell lysis, and were stained with Annexin V and 7AAD to measure the apoptosis using a commercial PE Annexin V Apoptosis Detection Kit I (BD559763). The cells were washed with ice-cold PBS and resuspended in 400 μL of binding buffer, and analyzed using a FACSCalibur flow cytometer.

Western blot

The lung tissue and peritoneal macrophages were lysed in ice-cold RIPA lysis buffer with 1% PMSF, and the homogenate was centrifuged at 12,000× g for 20 min at 4°C. Lysates were collected and the protein concentration was determined using the Enhanced BCA Protein Assay Kit (Beyotime P0010). Equal amounts of protein were transferred electrophoretically to NC membrane using a dry transfer method after the protein samples were dissociated by SDS-polyacrylamide gel. The NC membrane was sealed at room temperature for 3 h using BSA and incubated with an appropriate amount of diluted first antibody at 4°C overnight. The membrane was washed three times with the washing buffer, followed by the addition of secondary antibodies labeled with the appropriate alkaline phosphatase, and incubated at room temperature for 2 h. The membrane was washed three times with TBST, and analyzed using an enhanced chemiluminescene (ECL) Western blotting detection kit for HRP.

Statistical analysis

All the calculations were performed using SPSS13.0 and data charts using Prism 5.0 (GraphPad Software, USA). Measurement data were expressed as mean ± standard deviation (Mean ± SD). Statistical values were analyzed using one-way ANOVA, and pairwise comparison was conducted by SNK test. A *P*-value smaller than 0.05 (two-tailed) was considered statistically significant.

Results

Picroside II had a protective effect on mice with sepsis

The effect of picroside II on the mortality of mice with sepsis is illustrated in **Figure 1**. The

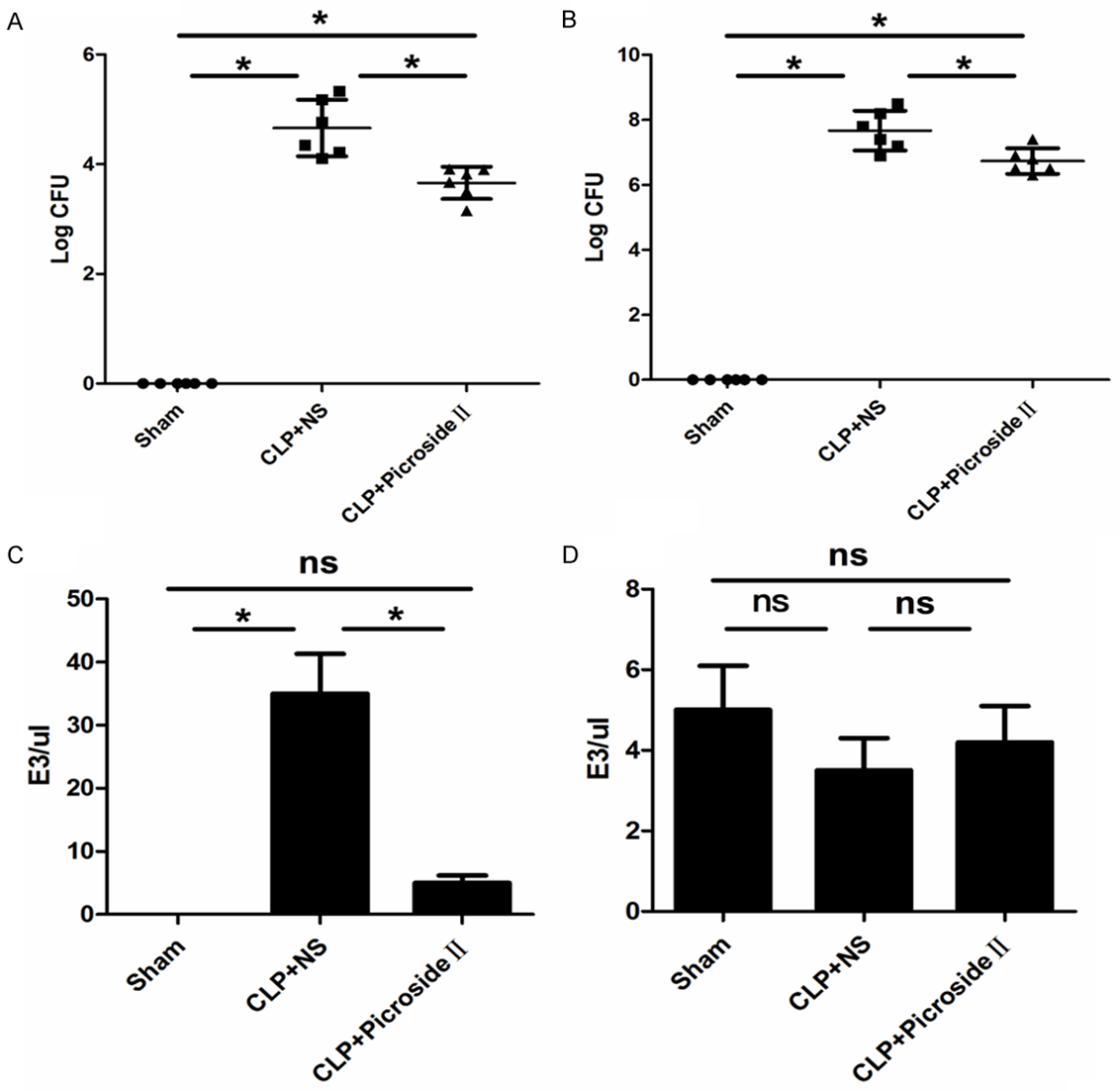

Figure 2. Picroside II treatment enhanced the ability of septic mice to remove bacteria. (A) Bacterial levels in peritoneal lavage fluid of the three groups at 24 h after CLP. (B) Bacterial levels in the peripheral blood of mice (six per group). The numbers of neutrophils gated by E3 in peritoneal lavage fluid (C) and peripheral blood (D) 24 h after CLP. All the values are expressed as mean ± sd. *, $P < 0.05$; ns, $P > 0.05$. All bars represent mean ± sd.

mice in the CLP+NS group showed a 10-day survival rate of 40%, while the mice in the CLP+Picroside II group achieved 60%, indicating that picroside II treatment significantly increased the survival rate in septic mice (60%, $P < 0.05$, **Figure 1A**).

Picroside II improved the lung injury of mice with sepsis, as shown in **Figure 2**. As is already known, lung is the primary target of organ damage in sepsis. The severity of lung injury in coagulation/anticoagulation imbalance, coagulation and pulmonary fibrin deposition, injury associated with alveolar epithelial cells and capillary endothelial cells, resulted in pulmonary interstitial and alveolar edema, and infiltration of a large number of inflammatory cells. HE staining of multiple inflammatory cells in the CLP+NS group showed alveolar infiltration, and severe alveolar wall destruction. Picroside II treatment decreased the infiltration and attenuated the lung injury associated with sepsis (**Figure 1B**). Compared with the sham group, the protein content of mice in the CLP+NS group was significantly increased, while the protein content of the CLP+picroside II mice in

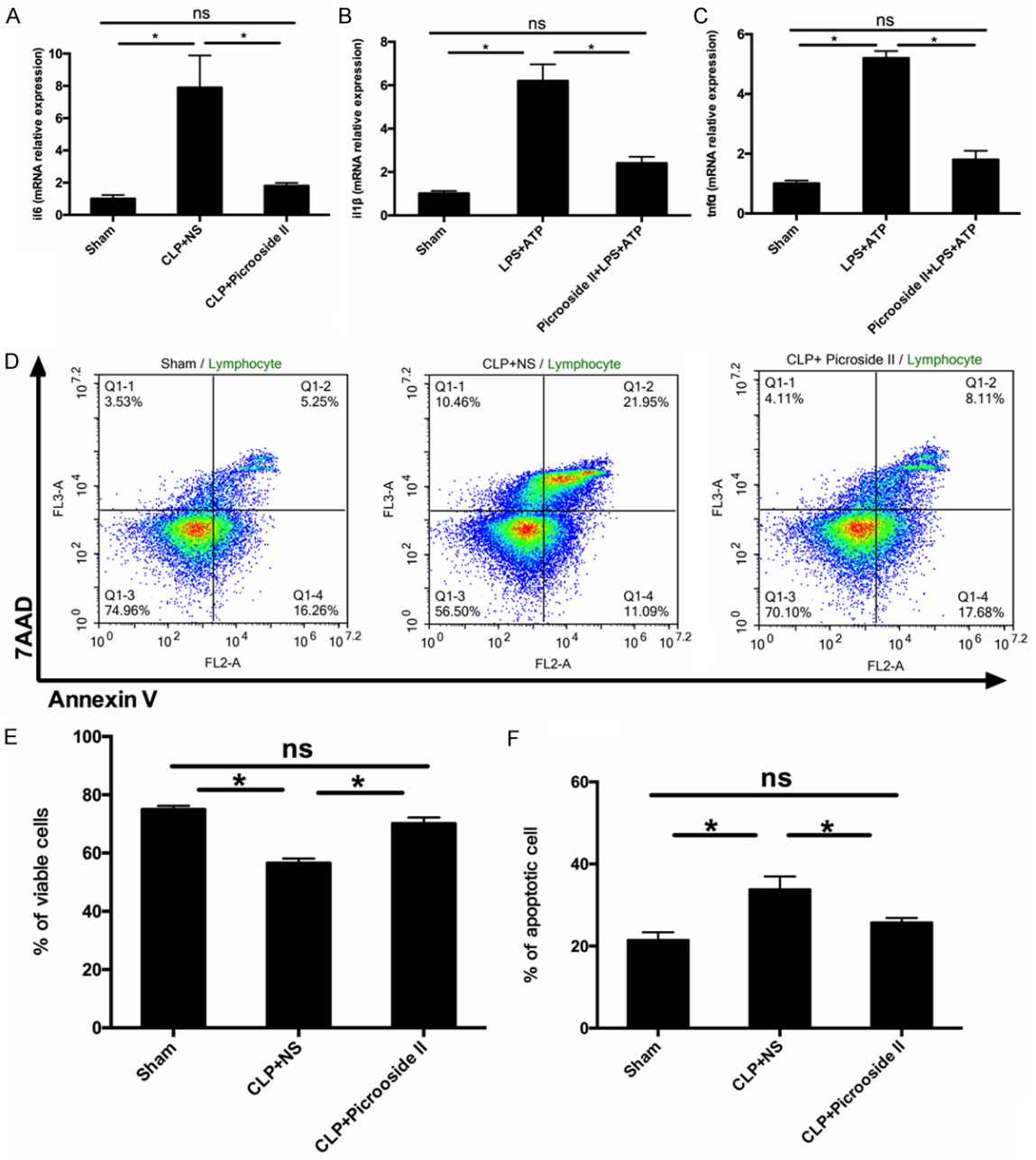

Figure 3. Picroside II treatment alleviated the inflammatory response in sepsis and enhanced immune function. Levels of IL-6 (A), IL-1β (B) and TNF-α (C) in the lung tissue of mice at 24 h after CLP (n = 6). (D) Lymphocytes were gated by physical map, and stained with Annexin V (FL2) and 7AAD (FL3). Histograms show rates of viability (E) and apoptosis (F) in the three groups. *, $P < 0.05$; ns, $P > 0.05$. All bars represent mean ± sd.

BALF was significantly lower than in the CLP+NS group (**Figure 1C**).

Picroside II treatment enhanced the antibacterial ability of septic mice

Sepsis is a systemic inflammatory response induced by infection. Studies have shown SIRS and organ damage following exposure to bacterial endotoxin, with the disease progression depending on the ability to clear bacteria. Nutrient agarose coating was used to detect differences in the number of bacteria in the peripheral blood and peritoneal lavage fluid. The results indicated that picroside II treatment significantly reduced the number of bacteria in

Table 1. Inflammatory cytokines (IL-6, IL-1β, TNF-α) associated with the peripheral blood of different groups of mice at 24 h after CLP

Group	IL-6 (pg/ml)	IL-1β (pg/ml)	TNF-α (pg/ml)
Sham	42.53±11.12#	35.61±6.25#	52.67±7.25#
CLP+NS	592.36±94.35*	267.57±21.31*	259.22±22.78*
CLP+Picroside II	289.53±42.94#	123.69±15.28#	169.35±15.82#

Note: *: P < 0.05, vs. sham group; #: P < 0.05, vs. CLP+NS.

the peritoneal lavage fluid (**Figure 2A**) and peripheral blood (**Figure 2B**) in mice at 24 h after CLP. Compared with the CLP+NS group, the picroside group showed a significant decrease in the number of neutrophils in the peritoneal lavage fluid (**Figure 2C**), while the difference in neutrophil count in the peripheral blood was not statistically significant (**Figure 2D**).

Picroside II treatment alleviated the inflammatory response

Picroside II improved inflammatory response, as shown in **Figure 3**. To explore whether picroside II further improved systemic inflammatory response and enhanced the bacterial clearance, we determined the IL-6, IL-1β and TNF-α levels in the peripheral blood and lung using ELISA. The results showed that picroside II treatment not only reduced the IL-6, IL-1β and TNF-α levels in peripheral blood of mice at 24 h after CLP (**Table 1**), but also reduced the inflammatory reaction in the lung (**Figure 3A-C**).

Picroside II inhibited apoptosis in spleen lymphocytes of septic mice and regulated immune function. Spleen cells from each of the three groups of mice were extracted and stained using Annexin V and 7AAD, and lymphocyte apoptosis was measured. It showed that apoptosis in the CLP+NS group was more serious compared with the sham group, while picroside II treatment reduced the degree of apoptosis and increased cell viability (**Figure 3D-F**).

Picroside II inhibited the host inflammatory response via NF-κB

We extracted total protein of lung tissue in mice from each group at 24 h after CLP, and determined the expression levels of p-NF-κB (p65) and IκB-α. We found that picroside II treatment reduced the expression of pNF-κB (p65) after CLP within 24 h, and enhanced the expression of IκB-α (**Figure 4A**). The mouse peritoneal macrophages were isolated and cultured *in vitro*, and divided into three groups: Group A (PBS), Group B (100 ng/mL LPS+PBS), and Group C (100 ng/mL LPS+500 μg/mL picroside II). The total protein was extracted from each group at 0 min, 30 min and 60 min, to determine the level of p-NF-κB (p65) and IκB-α, respectively. We found that picroside II significantly reduced the expression of p-NF-κB (p65) after LPS stimulation for 30 min, and enhanced the expression of IκB-α at the time points indicated (**Figure 4B**).

Picroside II inhibited the activation of NLRP3 inflammasome to reduce inflammatory response

NOD-LRRS containing pyrin domain 3 (NLRP3) is a members of the NLR (NOD-like receptor) family. NLRP3 inflammasome promotes the activation of caspase-1, maturation and secretion of IL-1β, and induces the expression and activation of a variety of cytokines associated with inflammatory cascade to produce immune responses. In order to investigate whether picroside II reduced the inflammatory response by modifying the activation of NLRP3 inflammasome, we isolated and cultured mouse macrophages *in vitro*, and constructed an activation model of NLRP3 inflammasome. We divided the macrophages into three groups: Group A (PBS), Group B (100 ng/mL LPS+1 mM ATP) and Group C (200 μg/mL picroside II+100 ng/mL LPS+1 mM ATP). Cell supernatant was collected from each group after 4 h, and the levels of IL-1β and caspase-1 were determined, respectively, and compared using ELISA. The total cellular protein was extracted after 18 h in each group, in which the expression of pro-caspase-1 and caspase-1 were detected and compared using Western blot. The results showed that picroside II treatment reduced the levels of IL-1β (**Figure 5A**) and caspase-1 (**Figure 5B**) in the cell supernatant significantly, without altering the expression of pro-caspase-1, while reducing the expression of caspase 1 (**Figure 5C**).

Discussion

Currently, sepsis is the principal cause of death in the intensive care unit (ICU) [27, 28]. The

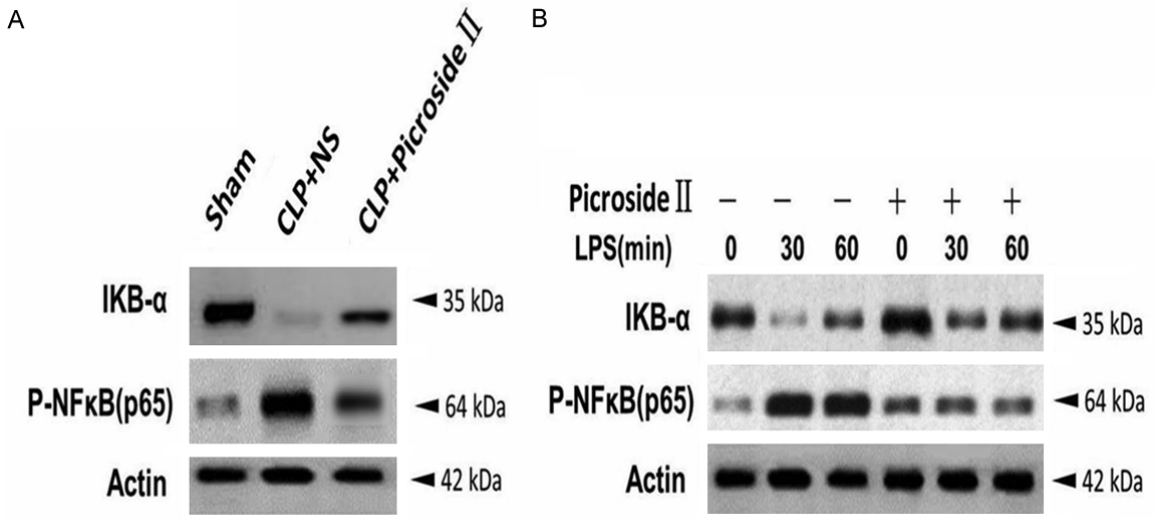

Figure 4. Picroside II inhibited the activation of inflammasome NLRP3 to reduce the inflammatory response. The expression level of p-NF-κB (p65) and IκB-α in the lung tissue of CLP model at 24 h (A) and at 0, 30, 60 min after LPS stimulation (B).

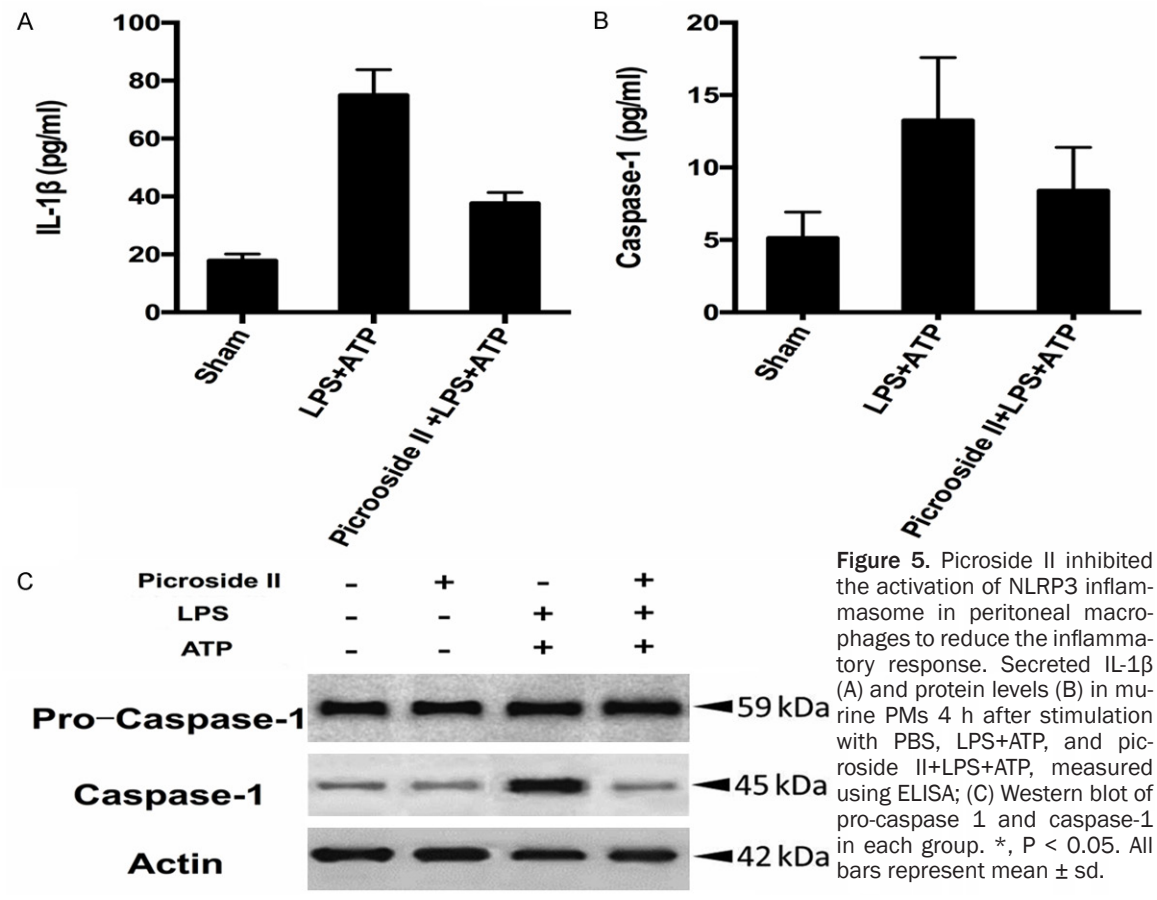

Figure 5. Picroside II inhibited the activation of NLRP3 inflammasome in peritoneal macrophages to reduce the inflammatory response. Secreted IL-1β (A) and protein levels (B) in murine PMs 4 h after stimulation with PBS, LPS+ATP, and picroside II+LPS+ATP, measured using ELISA; (C) Western blot of pro-caspase 1 and caspase-1 in each group. *, $P < 0.05$. All bars represent mean ± sd.

morbidity and mortality of sepsis remain high, despite advances in health care. Xigris, the only anti-septic drug approved by USA-FDA, has been withdrawn because of undetectable clinical effect [29]. Hence, it is crucial to explore effective drugs against sepsis.

Recent studies have shown that active ingredients such as iridoids play an important role against sepsis. Several effective components in Chinese medicine have been validated therapeutically in animal models of sepsis. Zheng et al. have found that geniposide, a type of cyclic polyether, has a protective effect in mice with sepsis *in vitro* [8]. Cao et al. found that arteannuin, a type of sesquiterpene lactone, alleviated the inflammatory response and oxidative damage in mice with sepsis [30]. Zhang et al. found that peoniflorin alleviated acute respiratory distress syndrome (ARDS) in patients with sepsis [31]. Picroside II has been validated for its anti-inflammatory, anti-oxidative and anti-apoptotic effects [32]. However, its anti-bacterial role in sepsis was not clear until now. CLP model is closely related to human models of sepsis induced by multiple pathogens, and is regarded as the gold standard for study of sepsis [33, 34].

Therefore, this study was based on the CLP model to explore the effect of picroside II on immune function in mice with sepsis. The results showed that picroside II increased the survival rate and reduced the degree of lung injury in mice of CLP model. Meanwhile, picroside II improved the immune function in mice with sepsis partially. The ability of peripheral blood and peritoneal cavity to clear bacteria is enhanced in septic mice. The excessive inflammatory responses were inhibited in mice with sepsis, including the release of inflammatory factors IL-6, IL-1β and TNF-α, and inhibition of chemotaxis and neutrophil infiltration in the peritoneal cavity, along with apoptosis in spleen lymphocytes. It may be associated with the activation of NF-κB and NLRP3 inflammasome, which are inhibited by picroside II.

A number of studies have shown that picroside II is a strong antioxidant and anti-inflammatory compound. For instance, picroside II exerted a a protective effect on mice in multiple ischemia reperfusion model. Further, it reduced the airway inflammation, inhibited bronchoconstriction, and exhibited anti-inflammatory and anti-asthmatic effects in asthmatic rats [35]. A few studies indicated that picroside II reduced the production of oxygen free radicals and repaired the cell membrane damage [36]. Wang T et al. found that picroside II reduced neutrophil infiltration in acute lung injury via TGF-β signaling pathway [37]. Wang L et al. found that picroside II downregulated the TLR4 and NF-κB signal transduction pathway and decreased the release of proinflammatory factors to prevent ischemia-reperfusion injury of mouse kidney [13].

Several results of this study were consistent with published studies. For example, picroside II injected into mouse tail vein decreased neutrophil infiltration in the peritoneal cavity of mice with sepsis, inhibited the activation of NF-κB, reduced the release of proinflammatory factors, and alleviated the degree of lung injury. The NLRs family of functional and structural pattern recognition receptor (PRRs) includes NOD1, NOD2 and NLRP3, which are similar to those of TLRs. NOD1 recognizes the components of the gram-negative bacteria cell wall. NOD2 binds to MDP, which is the degradation product of gram-positive and gram-negative bacteria, activates NF-κB and promotes cytokine expression including IL-1 and IL-18 by RIP2. During sepsis, pathogen-associated molecular patterns and risk-associated molecular patterns activated NLRP3 and caspase-1 to regulate the release of inflammatory cytokines such as IL18 and IL-1β, aggravating the inflammatory response [38]. This study showed that picroside II treatment inhibited the activation of NLRP3 in the peritoneal macrophages *in vitro*, which is consistent with amelioration of SIRS by picroside II.

Studies show that geniposide directly neutralized LPS in a dose-dependent manner *in vitro*, and reduced the level of LPS in the blood of the mouse model [8]. Picroside II enhances the ability of peripheral blood and peritoneal cavity to remove bacteria in septic mice probably by a similar mechanism.

Lymphocyte apoptosis may be one of the key factors underlying secondary immune suppression in sepsis, and may represent a marker of sepsis [39]. It plays a significant role in the pathophysiology of sepsis [40]. Studies using drugs to reduce lymphocyte apoptosis in mice with sepsis improved the survival rate [41]. Our study found that picroside II suppressed apoptosis in spleen lymphocytes of mice with sepsis. A large number of studies support the anti-apoptotic role of picroside II. For example, Deibert CP et al. found that picroside II inhibited neuronal apoptosis in brain ischemic injury

[42]. Wang L et al. showed that picroside II treatment decreased the apoptosis in lymphocytes of ischemia-reperfusion induced mouse renal injury model [43], which is consistent with our study.

It is well known that the excessive inflammatory response triggered by the pathogens is the direct cause of death in patients with sepsis [44]. Picroside II is an anti-inflammatory compound, which does not adversely affect host defense response. Its unique pharmacological mechanism may provide novel insight into the treatment of sepsis.

In summary, picroside II reduces the mortality of mice with sepsis, improves lung injury, decreases the release of proinflammatory factors and inhibits lymphocyte apoptosis in mouse spleen during sepsis. It alleviates the systemic inflammatory response triggered by sepsis by inhibiting the activation of NF-κB and NLRP3 inflammasome. The mouse CLP model demonstrates that picroside II exhibits a protective effect against sepsis.

Acknowledgements

This work was financially supported by the 12th Five-Year Key Project of PLA (No. BWS12J027), National Natural Science Foundation of China (No. 81372103), Natural Science Foundation of Shanghai (14ZR1413700), Open Projects of Jiangsu Province (KJS1403), and the Advanced Suitable Technology Popularization Project of Shanghai Health System (2013SY025).

Disclosure of conflict of interest

None.

Address correspondences to: Dr. Xueyin Shi, Jiangsu Province Key Laboratory of Anesthesiology and Jiangsu Province Key Laboratory of Anesthesia and Analgesia Application Technology, Xuzhou Medical University, Xuzhou 221002, China; Department of Anesthesiology, Xinhua Hospital Affiliated to Shanghai Jiaotong University School of Medicine, 1665 Kongjiang Road, Shanghai 200092, China; Department of Anesthesiology, Changzheng Hospital, Second Military Medical University, Shanghai, China. Tel: +86-21-25078712; Fax: +86-21-25078712; E-mail: shixueyin1128@163.com; Guo Xu, Department of General Surgery, Huai'an First People's Hospital, Nanjing Medical University, Huai'an, Jiangsu, China. Tel: +86-517-84922412; Fax: 86-517-80872266; E-mail: xg1167@163.com

References

[1] Shankar-Hari M, Phillips GS, Levy ML, Seymour CW, Liu VX, Deutschman CS, Angus DC, Rubenfeld GD and Singer M. Developing a new definition and assessing new clinical criteria for septic shock: for the third international consensus definitions for sepsis and septic shock (sepsis-3). JAMA 2016; 315: 775-787.

[2] Angus DC, Linde-Zwirble WT, Lidicker J, Clermont G, Carcillo J and Pinsky MR. Epidemiology of severe sepsis in the United States: analysis of incidence, outcome, and associated costs of care. Crit Care Med 2001; 29: 1303-1310.

[3] Coopersmith CM, Wunsch H, Fink MP, Linde-Zwirble WT, Olsen KM, Sommers MS, Anand KJ, Tchorz KM, Angus DC and Deutschman CS. A comparison of critical care research funding and the financial burden of critical illness in the United States. Crit Care Med 2012; 40: 1072-1079.

[4] Davis A, Henderson J and Langmack G. Development of an e-learning package for sepsis care. Br J Nurs 2016; 25: 292-296.

[5] Johnson K and Messier S. Early onset sepsis. S D Med 2016; 69: 29-33.

[6] Bopp C, Bierhaus A, Hofer S, Bouchon A, Nawroth PP, Martin E and Weigand MA. Bench-to-bedside review: The inflammation-perpetuating pattern-recognition receptor RAGE as a therapeutic target in sepsis. Crit Care 2008; 12: 201.

[7] Savva A and Roger T. Targeting toll-like receptors: promising therapeutic strategies for the management of sepsis-associated pathology and infectious diseases. Front Immunol 2013; 4: 387.

[8] Zheng XC, Yang D, Liu X, Wang N, Li B, Cao HW, Lu YL, Wei G, Zhou H and Zheng J. Study on the effective ingredient of gardenia in improving bacterial sepsis. Biochem and Mol Pharm Academic Meeting 2009; 59-59.

[9] Cao H, Guo Y, Wang N, Wei L, Wang J, Zhou H and Zheng J. Artemisinin protection of sepsis in rats. Acta Academ Med Milit Tert 2005; 27: 1769-1772.

[10] Zhang Q. The influence of paeoniflorin in TLR2 mediated the inflammatory response signal transduction pathways. J N Med Univer 2011.

[11] Li Q, Guo Y, Li Z and Xu X. The effects of glycosides II on the expression of Caspase-3 and PARP ischemia/reperfusion injury in rats. Chin Pharm Bull 2010; 26: 342-345.

[12] Zhang XD, Liu JW, Ting L and Yan C. Synergistic protective effect of picroside II and NGF on

PC12 cells against oxidative stress induced by H_2O_2. Pharm Rep Pr 2007; 59: 573-579.
[13] Wang L, Liu XH, Chen H, Chen ZY, Weng XD, Qiu T and Liu L. Picroside II protects rat kidney against ischemia/reperfusion-induced oxidative stress and inflammation by the TLR4/NF-κB pathway. Exp Ther Med 2015; 9: 1253-1258.
[14] He W and Lin J. Anti-inflammatory effect of glycosides II to asthma rats. J Chin Hosp 2005; 19: 233-235.
[15] Tak PP and Firestein GS. NF-kappaB: a key role in inflammatory diseases. J Clin Invest 2001; 107: 7-11.
[16] Clohisy JC, Hirayama T, Frazier E, Han SK and Abu-Amer Y. NF-κB signaling blockade abolishes implant particle-induced osteoclastogenesis. J Orthop Res 2004; 22: 13-20.
[17] Salminen A, Huuskonen J, Ojala J, Kauppinen A, Kaarniranta K and Suuronen T. Activation of innate immunity system during aging: NF-κB signaling is the molecular culprit of inflamm-aging. Ageing Res Rev 2008; 7: 83-105.
[18] Hawiger J, Veach RA and Zienkiewicz J. New paradigms in sepsis: from prevention to protection of failing microcirculation. J Thromb Haemost 2015; 13: 1743-1756.
[19] Yao Y and Sheng Z. Modern knowledge of signal transduction mechanism in sepsis. Crit Care Emerg Med 2003; 3-6.
[20] Guo H, Callaway JB and Ting JP. Inflammasomes: mechanism of action, role in disease, and therapeutics. Nat Med 2015; 21: 677-687.
[21] Lamkanfi M, Kanneganti TD, Franchi L and Nunez G. Caspase-1 inflammasomes in infection and inflammation. J Leukoc Biol 2007; 82: 220-225.
[22] Case CL. Regulating caspase-1 during infection: roles of NLRs, AIM2, and ASC. Yale J Biol Med 2011; 84: 333-343.
[23] Miao EA, Rajan JV and Aderem A. Caspase-1-induced pyroptotic cell death. Immunol Rev 2011; 243: 206-214.
[24] Shao BZ, Xu ZQ, Han BZ, Su DF and Liu C. NLRP3 inflammasome and its inhibitors: a review. Front Pharmacol 2015; 6: 262.
[25] Jo EK, Kim JK, Shin DM and Sasakawa C. Molecular mechanisms regulating NLRP3 inflammasome activation. Cell Mol Immunol 2016; 13: 148-159.
[26] Rittirsch D, Huber-Lang MS, Flierl MA and Ward PA. Immunodesign of experimental sepsis by cecal ligation and puncture. Nat Protoc 2009; 4: 31-36.
[27] Bermejo-Martin JF, Andaluz-Ojeda D, Almansa R, Gandia F, Gomez-Herreras JI, Gomez-Sanchez E, Heredia-Rodriguez M, Eiros JM, Kelvin DJ and Tamayo E. Defining immunological dysfunction in sepsis: A requisite tool for precision medicine. J Infect 2016; 72: 525-536.
[28] Delano MJ and Ward PA. Sepsis-induced immune dysfunction: can immune therapies reduce mortality? J Clin Invest 2016; 126: 23-31.
[29] ProCESS Investigators, Yealy DM, Kellum JA, Huang DT, Barnato AE, Weissfeld LA, Pike F, Terndrup T, Wang HE, Hou PC, LoVecchio F, Filbin MR, Shapiro NI, Angus DC. A randomized trial of protocol-based care for early septic shock. N Engl J Med 2014; 370: 1683-93.
[30] Cao H, Guo Y, Wei L, Wang N, Qu H and Zheng J. The effect of artemisinin on the rat liver lipid peroxidation damage in sepsis. Chin Clin Pharm Ther 2006; 11: 911-914.
[31] Zhang B, Li H, Wang Y, Wang F, Wang Y, Lv X, Qi R, Lu D and Wang H. The mechanism of paeoniflorin to reduce acute lung injury in sepsis mice. Chin J Pat 2011; 27: 1956-1960.
[32] Chen W, Li P, Yao Z, Wang B, Xue M and Xue L. Research progress of glycosides I and II. J Chin Med Mater 2015; 38: 1756-1760.
[33] Vasheghani F, Monemdjou R, Fahmi H, Zhang Y, Perez G, Blati M, St-Arnaud R, Pelletier JP, Beier F, Martel-Pelletier J and Kapoor M. Adult cartilage-specific peroxisome proliferator-activated receptor gamma knockout mice exhibit the spontaneous osteoarthritis phenotype. Am J Pathol 2013; 182: 1099-1106.
[34] Koufany M, Moulin D, Bianchi A, Muresan M, Sebillaud S, Netter P, Weryha G and Jouzeau JY. Anti-inflammatory effect of antidiabetic thiazolidinediones prevents bone resorption rather than cartilage changes in experimental polyarthritis. Arthritis Res Ther 2008; 10: R6.
[35] Li B, Zhang C, Fan X, Feng Q, Zhang L and Wu J. The research work based on the oxidation mechanism about pharmacological activity of picroside. Asia Pac Trad Med 2013; 9: 61-63.
[36] Rastogi R, Srivastava AK and Rastogi AK. Long term effect of aflatoxin B(1) on lipid peroxidation in rat liver and kidney: effect of picroliv and silymarin. Phytother Res 2001; 15: 307-310.
[37] Noh S, Ahn KS, Oh SR, Kim KH and Joo M. Neutrophilic lung inflammation suppressed by picroside II is associated with TGF-beta signaling. Evid Based Complement Alternat Med 2015; 2015: 897272.
[38] Abderrazak A, Syrovets T, Couchie D, El Hadri K, Friguet B, Simmet T and Rouis M. NLRP3 inflammasome: from a danger signal sensor to a regulatory node of oxidative stress and inflammatory diseases. Redox Biol 2015; 4: 296-307.
[39] Lang JD and Matute-Bello G. Lymphocytes, apoptosis and sepsis: making the jump from mice to humans. Crit Care 2009; 13: 109.

[40] Hotchkiss RS and Nicholson DW. Apoptosis and caspases regulate death and inflammation in sepsis. Nat Rev Immunol 2006; 6: 813-822.
[41] Hotchkiss RS, Coopersmith CM and Karl IE. Prevention of lymphocyte apoptosis--a potential treatment of sepsis? Clin Infect Dis 2005; 41 Suppl 7: S465-469.
[42] Deibert CP and Engh JA. Picroside II as a novel inhibitor of apoptosis after cerebral ischemia in rats. Neurosurgery 2015; 77: N17.
[43] Wang L, Liu X, Chen H, Chen Z, Weng X, Qiu T and Liu L. Effect of picroside II on apoptosis induced by renal ischemia/reperfusion injury in rats. Exp Ther Med 2015; 9: 817-822.
[44] Cavaillon JM, Adrie C, Fitting C and Adib-Conquy M. Reprogramming of circulatory cells in sepsis and SIRS. J Endotoxin Res 2005; 11: 311-320.